A&A 372, 527–534 (2001)
DOI: 10.1051/0004-6361:20010504

Astronomy & Astrophysics

HST observations of the LMC compact H II region N 11A⋆

M. Heydari-Malayeri[1], V. Charmandaris[2], L. Deharveng[3], M. R. Rosa[4,⋆⋆], D. Schaerer[5], and H. Zinnecker[6]

[1] DEMIRM, Observatoire de Paris, 61 avenue de l'Observatoire, 75014 Paris, France
[2] Cornell University, Astronomy Department, 106 Space Sciences Bldg., Ithaca, NY 14853, USA
[3] Observatoire de Marseille, 2 place Le Verrier, 13248 Marseille Cedex 4, France
[4] Space Telescope European Coordinating Facility, European Southern Observatory, Karl-Schwarzschild-Strasse-2, 85748 Garching bei München, Germany
[5] Observatoire Midi-Pyrénées, 14 avenue E. Belin, 31400 Toulouse, France
[6] Astrophysikalisches Institut Potsdam, An der Sternwarte 16, 14482 Potsdam, Germany

Received 13 March 2001 / Accepted 28 March 2001

Abstract. We present a study of the LMC compact H II region N 11A using *Hubble Space Telescope* imaging observations which resolve N 11A and reveal its unknown nebular and stellar features. The presence of a sharp ionization front extending over more than 4″ (1 pc) and fine structure filaments as well as larger loops indicate an environment typical of massive star formation regions, in agreement with high [O III]/Hβ line ratios. N 11A is a young region, as deduced from its morphology, reddening, and especially high local concentration of dust, as indicated by the Balmer decrement map. Our observations also reveal a cluster of stars lying towards the central part of N 11A. Five of the stars are packed in an area less than 2″ (0.5 pc), with the most luminous one being a mid O type star. N 11A appears to be the most evolved compact H II region in the Magellanic Clouds so far studied.

Key words. stars: early-type – ISM: dust, extinction – H II regions – ISM: individual objects: N 11A – galaxies: Magellanic Clouds

1. Introduction

The giant H II complex N 11 (Henize 1956) or DEM 34 (Davies et al. 1976) is the most luminous Hα source in the Large Magellanic Cloud (LMC) after the famous 30 Doradus (Kennicutt & Hodge 1986). Interestingly, N 11 has been suggested to be reminiscent of an evolved, some 2×10^6 years older version of the 30 Doradus starburst (Walborn & Parker 1992). Known also as MC 18 (McGee et al. 1972), it lies at the north-western extremity of the LMC bar and consists of a dozen ionized nebulae (named N 11A to N 11L) with several filaments surrounding a central cavity (see Fig. 1 of Rosado et al. 1996). Almost the entire complex is contained within a bubble $\sim 25' \times 20'$ (375 pc × 300 pc) in size created by stellar winds and several supernova explosions (Meaburn et al. 1989; Rosado et al. 1996; Mac Low et al. 1998; Kim et al. 1999). The complex harbors tens of hot stars at different stages of evolution distributed in four OB associations, LH 9, LH 10, LH 13, and LH 14 (Lucke & Hodge 1970).

A considerable amount of work has been devoted to examining various properties of the whole complex. In particular, the physical properties of the components B (LH 10), C (LH 13), and D (LH 14) and their massive star contents were studied by Heydari-Malayeri & Testor (1983 and 1985, hereafter Papers I and II), Heydari-Malayeri et al. (1987), Parker et al. (1992), Degioia-Eastwood et al. (1993), Heydari-Malayeri & Beuzit (1994), Parker et al. (1996), and Heydari-Malayeri et al. (2000). Parker et al. (1992) present an extensive spectral classification of some 70 O and B stars in the associations LH 9 and LH 10. The latter association, which powers N 11B, is the largest and brightest component of the complex containing several young massive stars of type O3.

N 11A (also known as IC 2116, HD 32279), to which this paper is devoted, is a quite isolated ionized region situated north-east of N 11B (see Fig. 1 of Paper I). It is a fairly bright object with $V \sim 12.5$ mag, and its size of $\sim$12″ makes it the smallest and the most compact nebula in the complex. Using ground-based narrow-band

Send offprint requests to: M. Heydari-Malayeri,
e-mail: heydari@obspm.fr

⋆ Based on observations with the NASA/ESA Hubble Space Telescope obtained at the Space Telescope Science Institute, which is operated by the Association of Universities for Research in Astronomy, Inc., under NASA contract NAS 5-26555.

⋆⋆ Affiliated to the Astrophysics Division, Space Science Department of the European Space Agency.

imaging and spectroscopy, in Papers I and II we studied several physical characteristics of N 11A (emission spectrum, excitation, extinction, gas density, chemical composition, abundances, etc.), and suggested that it is the most excited ionized region of the complex. These observations indicated that the excitation source has a $T_{\rm eff} \sim 44\,000$ K, corresponding to a mid-O type star. Israel & Koornneef (1991) also presented infrared and IRAS photometry of N 11A, and showed that it is a strong near-IR source dominated by nebular emission.

N 11A belongs to the class of the so-called high excitation blobs (HEBs) in the Magellanic Clouds. In contrast to the typical H II regions of the Magellanic Clouds, which are extended structures spread over several minutes of arc on the sky and powered by a large number of hot stars, HEBs are very dense small regions usually $5''$ to $10''$ in diameter. At the distance of the Magellanic Clouds this corresponds to sizes of more than 50 pc for normal H II regions and 1 to 3 pc for the blobs. They are also characterized by large amounts of local dust. HEBs are in fact created by very young massive stars just leaving their natal molecular cloud (see Heydari-Malayeri et al. 1999c for references).

In their study of N 11A, Parker et al. (1992) used a method for removing the contribution of the surrounding nebular brightness in CCD images and found an embedded star with $V = 14.21$ mag and two fainter neighbors (unpublished images). The presence of He II absorption lines in the spectrum of the brightest component (which they called LH 10: 3264) confirmed as O the spectral type of the main exciting source, even though contamination by very strong nebular emission lines made possible to only restrict its subclass within the O3–O5 V range.

In this paper we use the excellent imaging power of the *Hubble Space Telescope (HST)* to resolve N 11A and study the structure of the ionized gas as well as its stellar content. This allows us to present a clear picture of the compact ionized nebula and identify its exciting stars. Such information is essential for a better understanding of massive star formation, particularly in isolated, compact regions.

2. Observations and data reduction

The observations of N 11A were performed as part of our project GO-8247 with the Wide Field Planetary Camera 2 (WFPC2) on board of the *HST*. The images taken with the broad-band filters (F300W, F467M, F410M, and F547M) were obtained on February 7, 2000. Centered on the Planetary Camera (PC), these images had as a goal to reveal the details of the stellar content of N 11A. The narrow-band filter images (F487N, F503N and F656N) were obtained on May 21, 2000. In that case the target was centered on the WF2 which has larger pixels and lower noise than the PC CCD and is better suited for detecting faint nebular emission. Exposures were taken at 4 different pointings offset by $0''.8$ and the exposure times ranged from 10 to 300 s (see Table 1 for details).

Table 1. N 11A observations (*HST* GO-8247).

HST filter	Wavelength λ(Å)	Exposure time (s)
F300W (wide-U)	2911	$4 \times 14 = 56$
F410M (Strömgren v)	4090	$4 \times 50 = 200$
F467M (Strömgren b)	4669	$4 \times 35 = 140$
F547M (Strömgren y)	5479	$4 \times 10 = 40$
F487N (Hβ)	4866	$4 \times 260 = 1040$
F502N ([OIII])	5013	$4 \times 300 = 1200$
F656N (Hα)	6563	$4 \times 260 = 1040$

The data were processed through the standard *HST* pipeline calibration. Multiple images were co-added using the STSDAS task *imcombine*, while cosmic rays were detected and removed with the STSDAS task *crrej*. Normalized images were then created using the total exposure times for each filter. To extract the positions of the stars, the routine *daofind* was applied to the images by setting the detection threshold to 5σ above the local background level. The photometry was performed setting a circular aperture of 3–4 pixels in radius in the *daophot* package in STSDAS.

A crucial point in our data reduction was the sky subtraction. For most isolated stars the sky level was estimated and subtracted automatically using an annulus of 6–8 pixel width around each star. However, this could not be done for several stars located in the central region of N 11A due to their crowding. In those cases we carefully examined the PSF size of each individual star ($FWHM \sim 2$ pixels, corresponding to $0''.09$ on the sky) and did an appropriate sky subtraction using the mean of several nearby off-star positions. To convert into a magnitude scale we used zero points in the Vegamag system, that is, the system where Vega is set to zero mag in Cousin broad-band filters. The magnitudes measured were corrected for geometrical distortion, finite aperture size (Holtzman et al. 1995), and charge transfer efficiency as recommended by the *HST* Data Handbook. An additional correction to take into account the long versus short photometric anomaly (Casertano & Muchler 1998) was also applied. This increased the brightness of our fainter stars by as much as 0.4 magnitudes but it had no measurable effect on the brighter stars of the region.

We note that the filter F547M is wider than the standard Strömgren y filter. To evaluate the presence of any systematic effects in our photometry and color magnitude diagrams due to this difference in the filters, we used the STSDAS package *synphot*. Using synthetic spectra of hot stars, with spectral types similar to those found in H II regions, we estimated the difference due to the *HST* bandpasses to be less than 0.002 mag, which is well within the photometric errors.

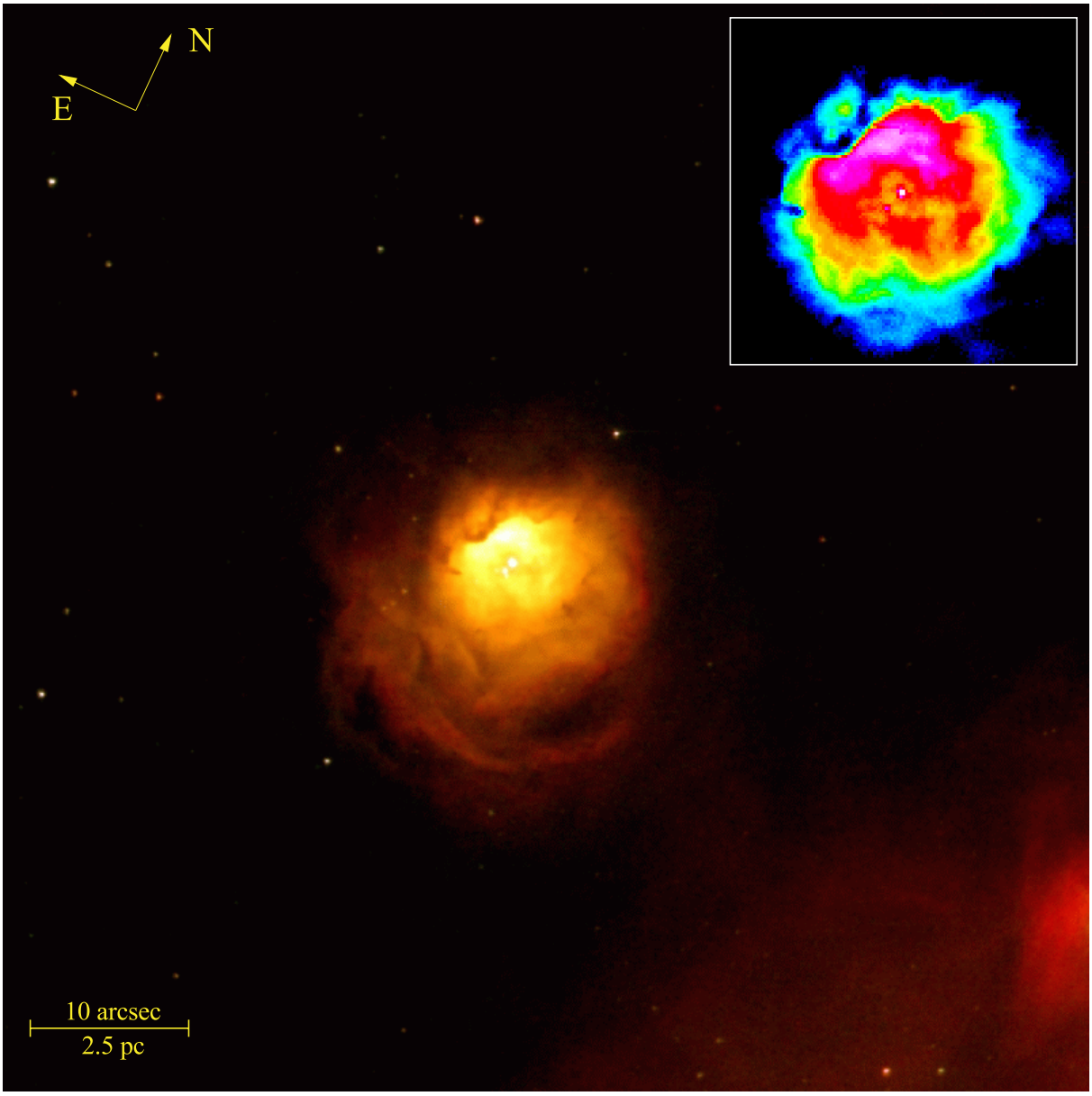

Fig. 1. A WFPC2 "true color" image of the LMC compact H II region N 11A created by combining images taken with the Hα (red), [O III] (green), and Hβ (blue) filters. The field size is $\sim$63″ × 63″ ($\sim$15 pc × 15 pc). The nebulosity to the south-west belongs to the large H II region N 11B. The false-color image shows N 11A in Hα.

3. Results

3.1. Morphology

Narrow-band Hβ and [O III] images obtained with ground-based telescopes show N 11B to be delineated at its eastern part by a sharp ionization front (Paper I). In those images N 11A appears as a featureless blob situated $\sim$50″ (12 pc) east of the ionization front.

The present *HST* observations resolve N 11A into a very bright core surrounded by a diffuse envelope of $\sim$8″ in diameter (Fig. 1) and reveal several interesting nebular and stellar features. A sharp ridge or front, extending over $\sim$4″ along the south-east to north-west direction, borders the core towards north. Beyond the ridge the Hα emission drops by about a factor of 10. A small cluster of five tightly packed stars are seen towards a cavity in the central region (Fig. 2).

The small scale filamentary structures are best seen in Fig. 3, which presents an un-sharp masking image of N 83B in Hα from which large scale structures have been subtracted. In order to remove these brightness variations and enhance the high spatial frequencies, a digital "mask" was created from the Hα image. First, the Hα image was convolved by a 2 × 2-pixel Gaussian, and then the smoothed frame was subtracted from the original Hα image.

3.2. Extinction and nebular emission

A map of the Hα/Hβ Balmer decrement is presented in Fig. 4a. It reveals a strong absorption zone north of the

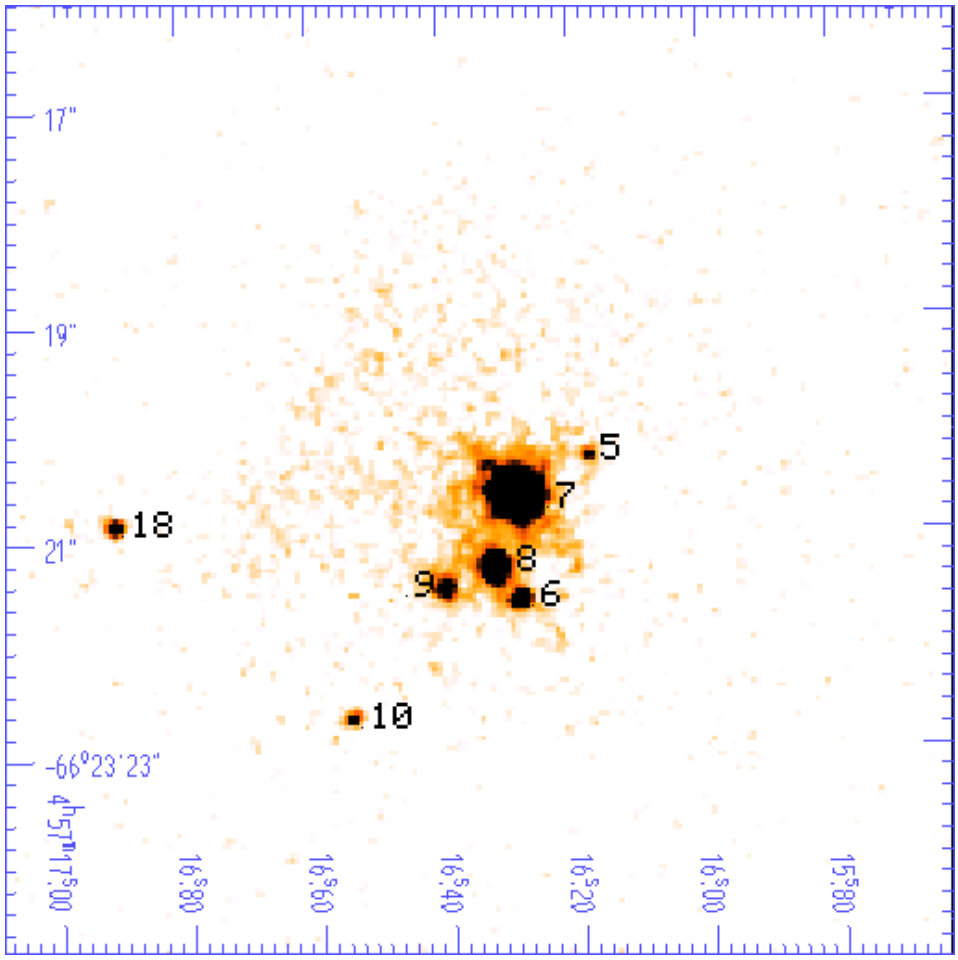

Fig. 2. The stellar content of the LMC compact H II region N 11A as revealed by the Strömgren y image. The field size $\sim 8''.8 \times 8''.8$ ($\sim 2.2\,\mathrm{pc} \times 2.2\,\mathrm{pc}$).

bright ridge, where the Hα/Hβ ratio reaches values as high as ∼5.5, while its mean value there is 4.5. Applying the interstellar reddening law, these ratios correspond to $A_V = 1.8$ and 1.3 mag respectively. Outside that area the ratio is smaller with a mean value of ∼3.5 which corresponds to $A_V = 0.6$ mag.

The [O III]λ5007/Hβ intensity map (Fig. 4b) reveals a remarkably extended high-excitation zone where the O^{++} ions occupy almost the same volume as H^+. The most excited area, though, surrounds the central stellar cluster, with a mean ratio of 4.1, while the ratio reaches slightly higher values in some pixels in the zone lying between the sharp ridge and the exciting stars. On average, the [O III]/Hβ is ∼3.7 over the diffuse part of the nebula.

Using the Hα/Hβ map, we can accurately correct the Hβ flux of the H II region for interstellar reddening on a pixel by pixel basis. The total corrected flux is $F_0(\mathrm{H}\beta) = 1.17 \times 10^{-11}$ erg cm^{-2} s^{-1} above 3σ level without the stellar contribution and accurate to 3%, if our extinction correction which assumes external dust is verified. Supposing that the H II region is ionization-bounded, the corresponding Lyman continuum flux of the region is $N_{\mathrm{L}} = 9.10 \times 10^{48}$ photons s^{-1}. Similarly, with the assumption of a homogeneous spherical nebula, a mean electron density of 550 cm^{-3} can be derived from the Hβ flux, which leads to an ionized hydrogen mass estimate of 54 $M_\odot$.

A single main sequence star of type O7.5 or O8 or several massive stars of later types can account for this ionizing photon flux (Vacca et al. 1996; Schaerer & de Koter 1997). However, this could clearly be an underestimate since the H II region is more likely to be density-bounded almost in all directions except northward where lies the sharp ridge.

3.3. Stellar content

The automatic search routine *daofind* detected 18 stars in the WFPC2 field of N 11A, all of them unambiguously present in the four stellar filters (Fig. 5) with their magnitudes ranging from $y = 14.69$ to 20.23. The photometry measurements for these stars are presented in Table 2, where the star numbers refer to Figs. 2 and 4.

Among these stars only seven are situated in the direction of N 11A. A small cluster of five stars, observed at the center of N 11A (Fig. 2), is obviously associated with this region. Star #7, with a y magnitude of 14.69 is the main exciting star of the region, nearly 6 times more luminous

Table 2. Photometry of the brightest stars towards N 11A.

Star	RA (J2000)	Dec (J2000)	F300W Wide U	F410M Strömgren v	F467M Strömgren b	F547M Strömgren y	Color $b-y$
1	4:57:13.9	–66:23:21.0	18.74	19.30	19.47	19.29	+0.18
2	4:57:14.7	–66:23:07.4	18.94	19.32	19.31	19.51	–0.20
3	4:57:15.4	–66:23:35.7	18.38	19.36	19.42	19.40	+0.02
4	4:57:15.9	–66:23:10.2	14.52	16.02	16.13	16.15	–0.02
5	4:57:16.2	–66:23:20.3	–	–	–	20.23	–
6	4:57:16.3	–66:23:21.6	17.03	18.28	18.34	18.26	+0.08
7	4:57:16.3	–66:23:20.6	12.85	14.59	14.67	14.69	–0.02
8	4:57:16.3	–66:23:21.3	15.16	16.70	16.67	16.68	–0.01
9	4:57:16.4	–66:23:21.5	17.56	18.68	18.81	18.68	+0.13
10	4:57:16.6	–66:23:22.7	18.13	19.92	19.27	19.41	–0.14
11	4:57:17.2	–66:23:25.2	17.75	19.21	19.28	19.32	–0.04
12	4:57:17.3	–66:23:26.3	18.81	19.26	19.19	19.31	–0.11
13	4:57:17.3	–66:23:26.8	18.22	19.15	19.13	19.14	–0.01
14	4:57:17.4	–66:23:20.7	18.45	19.26	19.23	19.32	–0.09
15	4:57:17.4	–66:23:09.3	18.48	19.56	19.50	19.54	–0.04
16	4:57:17.7	–66:23:18.3	19.18	19.31	19.34	19.38	–0.04
17	4:57:18.5	–66:23:18.8	17.26	18.46	18.40	18.50	–0.10
18	4:57:16.9	–66:23:20.9	17.39	19.32	18.81	18.88	–0.07

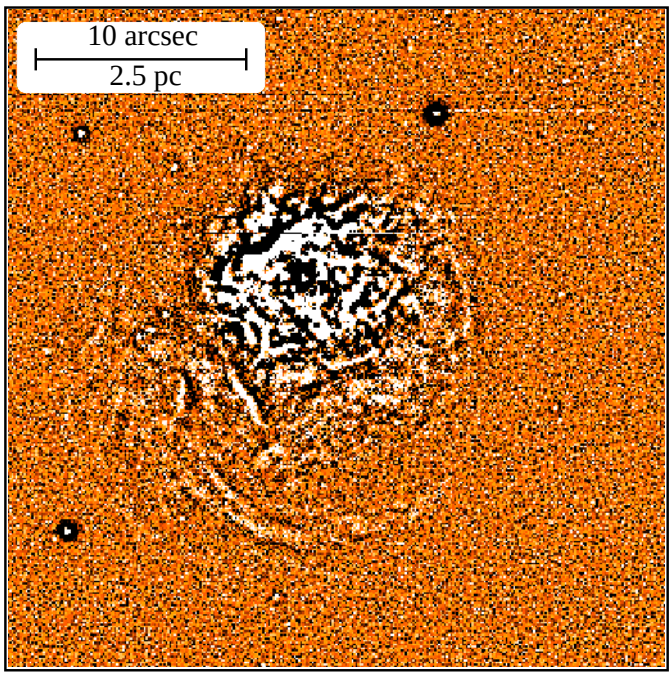

Fig. 3. An un-sharp masking image of N 11A obtained in Hα, which highlights the filamentary patterns of the nebula (see the text). The field size is $\sim 30'' \times 30''$ (7.5 pc × 7.5 pc), and the orientation as in Fig. 1.

than star #8, the second brightest star, which is situated $\sim 0''.7$ to its south, and has a magnitude of $y = 16.68$. Star #5 lying $0''.8$ to the north-east of #7 is the faintest member of the sample. If this one is an exciting star, its faint magnitude should be due to local reddening.

One could try to estimate the luminosity of the brightest star of the cluster (#7), although in the absence of spectroscopic data this is not accurate. Using an extinction of $A_V = 0.6$ mag corresponding to the mean value for the associated nebula (Sect. 3.2), and a distance modulus $m - M = 18.5$ (e.g. Kovács 2000 and references therein), we find a visual absolute magnitude $M_V = -4.4$. If the star is on the main sequence, it would be an O9V according to the calibration of Vacca et al. (1996) for Galactic stars. Its corresponding luminosity and mass would be $\log L = 5.06\ L_\odot$ and $M = 25\ M_\odot$.

Parker et al. (1992) derived a more luminous exciting star with $M_V = -5.1$ mag corresponding to an O6V type. The reason for this discrepancy is that they measure a V magnitude which is 0.48 mag brighter than our Strömgren y and also use a stronger visual extinction of $A_V = 0.8$ mag. A magnitude offset of this type could be attributed to the fact that the exciting stars are tightly packed inside a very bright H II region, making sky subtraction difficult.

4. Discussion

The total Hβ flux measured for N 11A corresponds to a main exciting source of spectral type O7.5–O8V. There are two major reasons, though, which suggest that this estimate is a lower limit to the power of the exciting star. One, as we mentioned earlier, is the fact that the H II region is most probably not fully ionization-bounded and a fraction of the UV photons produced by the star remain unaccounted for because they escape into the interstellar medium. A second factor which contributes to underestimating the Hβ flux is possibly an inadequate estimate of the extinction correction, since the Hβ flux was corrected assuming only external extinction. Otherwise, it is also probable that the region harbors hotter undetected stars still embedded in the gas/dust concentrations. The same exciting star was observed by Parker et al. (1992) who estimated its spectral type as O6-O3V. The O3 type, though, is uncertain because of contamination by the strong

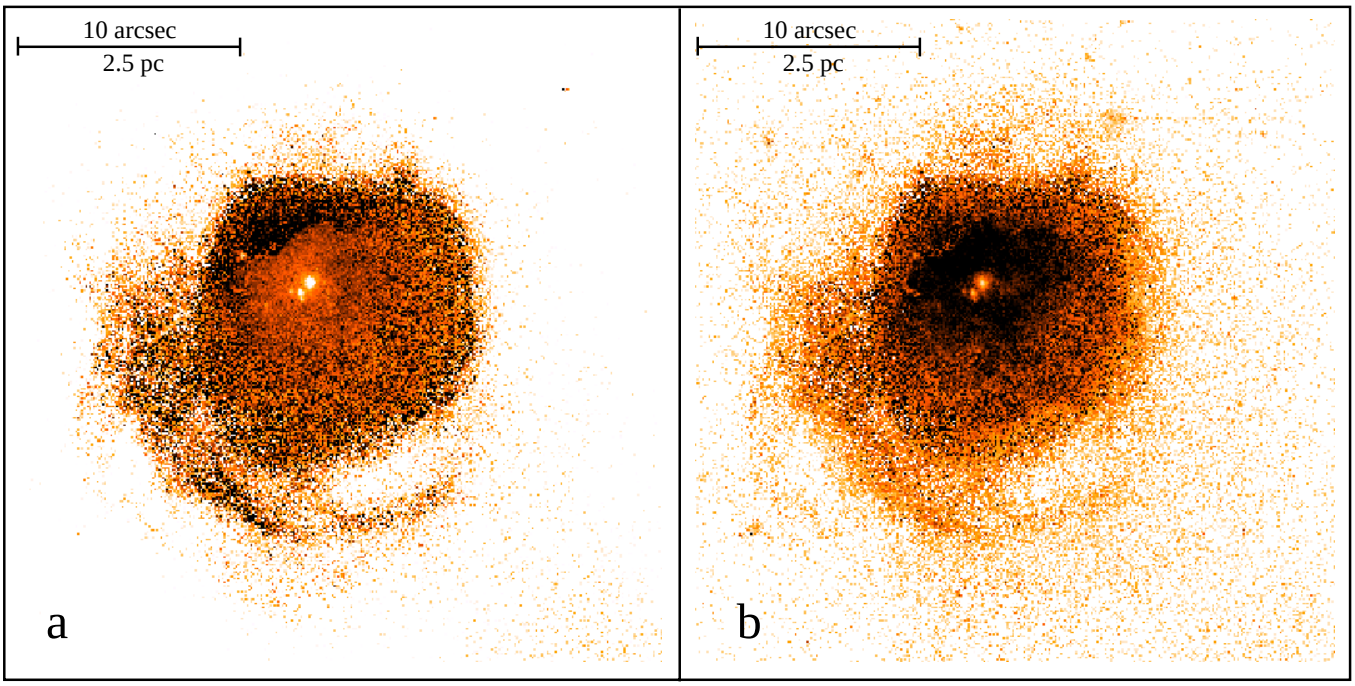

Fig. 4. Line intensity ratios for the LMC compact nebula N 11A. Darker colors correspond to higher ratio values. The field of view and orientation are identical to Fig. 3. The white spots are stars and can be identified using Fig. 2. **a)** Hα/Hβ Balmer decrement. Its mean value over the diffuse component is $\sim$3.5 ($A_V = 0.6$ mag), while the ratio goes up to $\sim$5.5 ($A_V = 1.8$ mag) towards the darkest area north-east of the exciting stars. **b)** The [O III]λ5007/Hβ ratio. The mean value around the stars is 4.1, while the highest values reach $\sim$4.5 in the zone between the exciting stars and the sharp ridge.

nebular emission line of He I λ 4471 Å. Moreover, if an O3V star lies inside N 11A, one would expect an [O III]/Hβ ratio much higher than that actually measured.

Ionization fronts in H II regions, which represent the separation between the hot ionized gas and the photodissociation region, can appear differently according to their orientation with respect to the line of sight. The high resolution *HST* images reveal a sharp ridge north-east of the exciting stars which can be explained by the presence of such a front. The associated molecular cloud in which the stars of N 11A formed must therefore be further to the north-east of that front, in agreement with the observation that the dust content increases significantly in that direction, as suggested by the higher values of the Balmer decrement. This result is supported by the CO (1–0) observations of the N 11 complex (Israel & de Graauw 1991; Caldwell & Kutner 1996). The CO map shows that molecular emission comes from a zone surrounding the central cavity of N 11 and has a long branch spreading in a north-east direction which passes by N 11A. Although the spatial resolution of the CO map is much coarser than that of the present observations, there is little doubt about the relative position of the molecular cloud with respect to N 11A.

The morphology of N 11A is well accounted for by the champagne model (Tenorio-Tagle 1979; Bodenheimer et al. 1979). It corresponds to the evolutionary stage when the ionization front has reached the border of the molecular cloud. The central bright area (Fig. 1) is the cavity created in the molecular cloud by the ionizing photons of the stars, and the bright ridge is a part of the cavity situated along the line of sight. Dense ionized gas is pouring out of the cavity into the interstellar medium as shown by the presence of the outer diffuse component. Since the line of sight is slightly tilted with respect to the outflow axis, a part of the cavity and the associated external dust hides a portion of the H II region and causes the higher extinction observed at its north-east side. The surrounding filamentary structure (Fig. 3) is probably created by the stellar winds from the central cluster acting on the dense ionized gas at the surface of the molecular cloud.

The compact H II region N 11A is the fifth in a sample of HEBs we have observed so far with *HST*. The other regions of the sample are N 159-5 (the Papillon nebula) and N 83B in the LMC (Heydari-Malayeri et al. 1999c, 2001), as well as N 81 and N 88A in the SMC (Heydari-Malayeri et al. 1999a, 1999b). Despite the small number of regions available, it would be interesting to compare those HEBs by examining a possible correlation between their de-reddened Hβ fluxes and the corresponding [O III] (5007 Å)/Hβ ratios (Fig. 6). The motivation for that is due to current photoionization models of spherically symmetric H II regions which suggest that the emission line spectrum of the region depends on the effective temperature of the star(s), the ionization parameter, and the gas metallicity (Stasińska 1990; Stasińska & Leitherer 1996). The ionization parameter is defined as

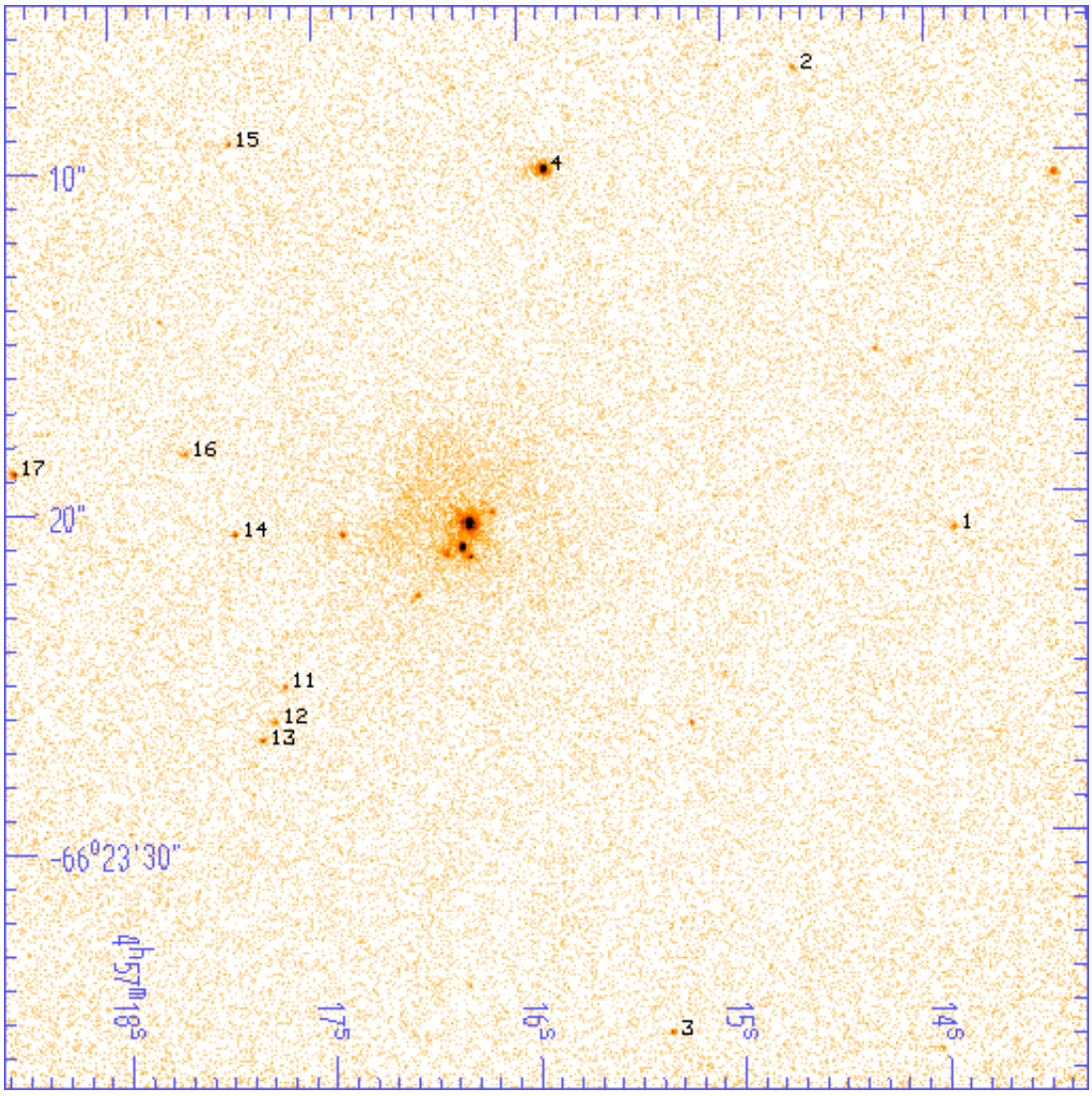

Fig. 5. A WFPC2 image showing the LMC compact H II N 11A and its adjacent field in the Strömgren y filter (F547M) where the brighter stars are labelled. A close-up image of the H II region is displayed in Fig. 2 and the photometry of the stars is presented in Table 2. The field size is $\sim 32'' \times 32''$ ($\sim 8\,\mathrm{pc} \times 8\,\mathrm{pc}$), and the coordinates are in J2000.

$U = Q/4\pi R^2 nc$, where Q is the total number of ionizing photons with energy above 13.6 eV, R the Strömgren radius, n the hydrogen density, and c the speed of light. Models by Stasińska (1990) show a linear correlation between [O III]/Hβ and the Hβ flux for H II regions with the same gas density, the same number of exciting stars, but with increasing effective temperatures. The reason for this relationship is that when there are energetic UV photons available for producing high [O III] /Hβ ratios, they also produce a large Hβ flux. The models also show that lower metallicity environments favor higher [O III]/Hβ ratios, but the metallicity dependence can be outweighed by the ionization parameter.

Even though the real H II regions are not ionization-bounded spheres, and one should be careful when applying model results to observations; the fact that HEBs have sizes which are of the same order of magnitude provides a good opportunity for comparison. It is interesting that if we exclude N 159-5, the plot of Fig. 6 suggests that there is indeed a linear relationship as predicted by the models. The reason for discarding N 159-5 is because we know (Heydari-Malayeri et al. 1999c) that it is a very reddened region by both local and external dust, and its discrepant position may be due to inadequate flux correction for extinction in a manner similar to the one discussed at the beginning of this section. If our reasoning is justified, then the measured Hβ flux of N 159-5 is underestimated by a factor of $\sim$5, mainly due to the effect of internal dust whose properties remain to be studied. We also observe that among the HEBs studied, SMC N 88A is the most excited and LMC N 11A the least excited. The lower excitation of N 11A may simply be due to the fact that it is excited by a less massive, young star. It may also be the result of an evolutionary effect, in the sense that

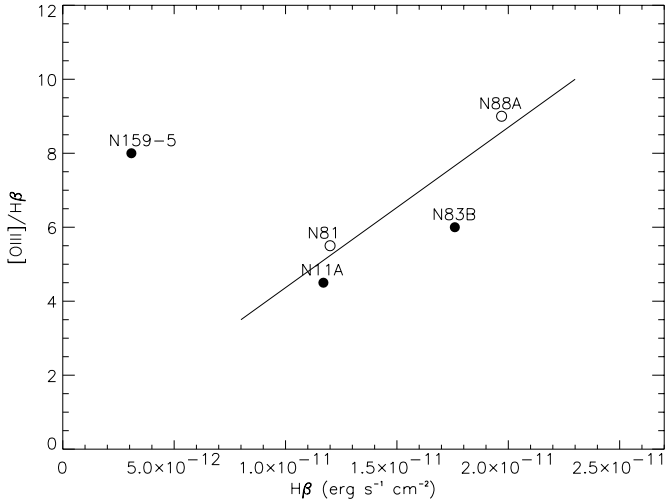

Fig. 6. The variation of the [O III] (5007 Å)/Hβ ratio for the Magellanic Clouds compact H II regions with respect to their corresponding de-reddened Hβ flux. The full dots denote the LMC regions and the empty dots SMC ones. The line is simply indicative of the direction of the correlation suggested by the models.

the lower [O III]/Hβ may in fact be the consequence of a smaller gas density caused by the champagne outflow. From our previous *HST* observations we know that SMC N 88A is younger than SMC N 81, since it is more compact, of higher gas density, and more affected by dust so that its exciting stars are still hidden inside the H II region. The same holds for the LMC objects, since N 159-5 is associated with a much larger amount of dust than N 83B and N 11A and is more compact compared to them.

One should keep in mind though, that despite the compactness of N 11A (and HEBs in general) compared to typical extragalactic H II regions, if it was situated in our Galaxy, it would appear as a rather "classical" H II region nearly ∼4 times smaller than the Orion nebula. In fact, based on our new observation, it appears that N 11A has many similarities with Orion regarding its central exciting cluster, its high excitation, a region of high extinction at the northern border and the filamentary loops on the southern side. Consequently, these small, high excitation, compact H II regions found in the Magellanic Clouds near locations where other giant H II regions are present, are very interesting to study in order to better understand massive star formation processes in more distant galaxies.

Acknowledgements. We would like to thank the referee Dr. Joel Wm. Parker for his helpful comments. We are also grateful to Dr. Grażyna Stasińska for discussions. VC would like to acknowledge the financial support for this work provided by NASA through grant number GO-8247 from the STScI, which is operated by the Association of Universities for Research in Astronomy, Inc., under NASA contract 26555.

References

Bodenheimer, P., Tenorio-Tagle, G., & Yorke, H. W. 1979, ApJ, 233, 85
Caldwell, D. A., & Kutner, M. L. 1996, ApJ, 472, 611
Casertano, S., & Muchler, M. 1998, Instrument Science Report WFPC2 98-02
Davies, R. D., Elliott, K. H., & Meaburn, J. 1976, MNRAS, 81, 89
Degioia-Eastwood, K., Meyers, R. P., & Jones, D. P. 1993, AJ, 106, 1005
de Koter, A., Heap, S. R., & Hubney, I. 1997, ApJ, 477, 792
Henize, K. G. 1956, ApJS, 2, 315
Heydari-Malayeri, M., & Beuzit, J.-L. 1994, A&A, 287, L17
Heydari-Malayeri, M., & Testor, G. 1983, A&A, 118, 116 (Paper I)
Heydari-Malayeri, M., & Testor, G. 1985, A&A, 144, 98 (Paper II)
Heydari-Malayeri, M., Niemela, V., & Testor, G. 1987, A&A, 184, 300
Heydari-Malayeri, M., Rosa, M., Zinnecker, H., Deharveng, L., & Charmandaris, V. 1999a, A&A, 344, 848
Heydari-Malayeri, M., Charmandaris, V., Deharveng, L., Rosa, M. R., & Zinnecker, H. 1999b, A&A, 347, 841
Heydari-Malayeri, M., Rosa, M. R., Charmandaris, V., Deharveng, L., & Zinnecker, H. 1999c, A&A, 352, 665
Heydari-Malayeri, M., Royer, P., Rauw, G., & Walborn, N. R. 2000, A&A, 361, 877
Heydari-Malayeri, M., Charmandaris, V., Deharveng, L., et al. 2001, A&A, 372, 495
Holtzman, J., Hester, J. J., Casertano, S., et al. 1995, PASP, 107, 156
Israel, F. P., & de Graauw, Th. 1991, The Magellanic Clouds, ed. R. Hanes, & D. Milne, IAU Symp. 148, 45
Israel, F. P., & Koornneef, J. 1991, A&A, 248, 404
Kennicutt, R. C., & Hodge, P. W. 1986, ApJ, 306, 130
Kim, S., Dopita, M. A., Staveley-Smith, L., & Bessell, M. S. 1999, AJ, 118, 2797
Kovács, G. 2000, A&A, 363, L1
Lucke, B. P., & Hodge, P. W. 1970, AJ, 75, 171
Mac Low, M.-M., Chang, T. H., Chu, Y.-H., et al. 1998, ApJ, 493, 260
McGee, R. X., & Newton, L. M. 1972, Aust. J. Phys., 25, 619
Meaburn, J., Solomos, N., Laspias, V., & Goudis, C. 1989, A&A, 225, 497
Parker, J. Wm., Garmany, C. D., Massey, P., & Walborn, N. R. 1992, AJ, 103, 1205
Parker, J. Wm., Hill, J. K., Bohlin, R. C., et al. 1996, ApJ, 472, L29
Relyea, L. J., & Kurucz, R. L. 1978, ApJS, 37, 45
Rosado, M., Laval, A., Le Coarer, E., et al. 1996, A&A, 308, 588
Schaerer, D., & de Koter, A. 1997, A&A, 322, 598
Stasińska, G. 1990, A&AS, 83, 501
Stasińska, G., & Leitherer, C. 1996, ApJS, 107, 661
Tenorio-Tagle, G. 1979, A&A, 71, 79
Vacca, W. D., Garmany, C. D., & Shull, J. M. 1996, ApJ, 460, 914
Walborn, N. R., & Parker, J. Wm. 1992, ApJ, 399, L87